Deep-Sea Research II 55 (2008) 1684–1695

Contents lists available at ScienceDirect

Deep-Sea Research II

journal homepage: www.elsevier.com/locate/dsr2

In situ measurement of mesopelagic particle sinking rates and the control of carbon transfer to the ocean interior during the Vertical Flux in the Global Ocean (VERTIGO) voyages in the North Pacific

T.W. Trull [a,b,c,*], S.G. Bray [a], K.O. Buesseler [d], C.H. Lamborg [d], S. Manganini [d], C. Moy [a], J. Valdes [d]

[a] Antarctic Climate and Ecosystems Cooperative Research Centre (ACE CRC), Hobart, Tasmania 7001, Australia
[b] Commonwealth Scientific and Industrial Research Organisation (CSIRO), Marine and Atmospheric Research, Hobart, Tasmania 7001, Australia
[c] University of Tasmania Institute of Antarctic and Southern Ocean Studies, Hobart, Tasmania 7001, Australia
[d] Woods Hole Oceanographic Institution, Woods Hole, MA 02543, USA

ARTICLE INFO

Article history:
Accepted 16 April 2008
Available online 13 May 2008

Keywords:
Mesopelagic
Sinking rate
Settling velocity
Particle flux
Sediment trap
North Pacific

ABSTRACT

Among the parameters affecting carbon transfer to the ocean interior, particle sinking rates vary three orders of magnitude and thus more than primary production, *f*-ratios, or particle carbon contents [e.g., Boyd, P.W., Trull, T.W., 2006. Understanding the export of marine biogenic particles: is there consensus? Progress in Oceanography 4, 276–312, doi:10.1016/j.pocean.2006.10.007]. Very few data have been obtained from the mesopelagic zone where the majority of carbon remineralization occurs and the attenuation of the sinking flux is determined. Here, we report sinking rates from ~300 m depth for the subtropical (station ALOHA, June 2004) and subarctic (station K2, July 2005) North Pacific Ocean, obtained from short (6.5 day) deployments of an indented rotating sphere (IRS) sediment trap operating as an *in situ* settling column [Peterson, M.L., Wakeham, S.G., Lee, C., Askea, M.A., Miquel, J.C., 2005. Novel techniques for collection of sinking particles in the ocean and determining their settling rates. Limnology and Oceanography Methods 3, 520–532] to separate the flux into 11 sinking-rate fractions ranging from >820 to $>2\,m\,d^{-1}$ that are collected by a carousel for further analysis.

Functioning of the IRS trap was tested using a novel programming sequence to check that all particles have cleared the settling column prior to the next delivery of particles by the 6-hourly rotation cycle of the IRS. There was some evidence (from the flux distribution among the cups and photomicroscopy of the collected particles) that very slow-sinking particles may have been under--collected because they were unable to penetrate the brine-filled collection cups, but good evidence for appropriate collection of fast-settling fractions.

Approximately 50% of the particulate organic carbon (POC) flux was sinking at greater than $100\,m\,d^{-1}$ at both stations. At ALOHA, more than 15% of the POC flux sank at $>820\,m\,d^{-1}$, but low fluxes make this uncertain, and precluded resolution of particles sinking slower than $137\,m\,d^{-1}$. At K2, less than 1% of the POC flux sank at $>820\,m\,d^{-1}$, but a large fraction (~15–45%) of the flux was contributed by other fast-sinking classes (410 and $205\,m\,d^{-1}$). PIC and BSi minerals were not present in higher proportions in the faster sinking fractions, but the observations were too limited to rule out a ballasting contribution to the control of sinking rates. Photographic evidence for a wide range of particle types within individual sinking-rate fractions suggests that biological processes that set the porosity and shape of particles are also important and may mask the role of minerals.

Comparing the spectrum of sinking rates observed at K2 with the power-law profile of flux attenuation with depth obtained from other VERTIGO sediment traps deployed at multiple depths [Buesseler, K.O., Lamborg, C.H., Boyd, P.W., Lam, P.J., Trull, T.W., Bidigare, R.R., Bishop, J.K.B., Casciotti, K.L., Dehairs, F., Elskens, M., Honda, M., Karl, D.M., Siegel, D., Silver, M., Steinberg, D., Valdes, J., Van Mooy, B., Wilson, S.E., 2007b. Revisiting carbon flux through the Ocean's twilight zone. Science 316(5824), 567–570, doi: 10.1126/science.1137959] emphasizes the importance of particle transformations within the mesopelagic zone in the control of carbon transport to the ocean interior.

* Corresponding author at: Antarctic Climate and Ecosystems Cooperative Research Centre (ACE CRC), Hobart, Tasmania 7001, Australia. Tel.: +61 3 62 262988; fax: +61 3 62 262973.
E-mail address: Tom.Trull@utas.edu.au (T.W. Trull).

0967-0645/$ - see front matter © 2008 Elsevier Ltd. All rights reserved.
doi:10.1016/j.dsr2.2008.04.021

1. Introduction

Sinking particles structure ocean ecosystems. They cause the oligotrophic conditions that characterize most of the global ocean surface, induce chemical gradients that significantly reduce atmospheric carbon dioxide (Broecker and Takahashi, 1978; Volk and Hoffert, 1985; Sarmiento and Orr, 1991), couple pelagic and benthic ecosystems (Deuser, 1996; Jahnke, 1996), and provide a fast path for anthropogenic pollutants to reach the deep sea (Fowler and Knauer, 1986). As the particles sink they are rapidly remineralized, so that typically less than 10% of the particulate organic carbon leaving the surface reaches the deep sea (deeper than 1000 m) and less than 1% reaches abyssal sediments (Suess, 1980; Martin et al., 1987; Honjo, 1996; Jahnke, 1996; Oschlies and Kahler, 2004).

The attenuation of carbon flux with depth represents a balance between particle properties that aid transit (e.g., fast-sinking rates, protection of organic matter within minerals, aggregation) and those that retard it (e.g., slow-sinking rates, disaggregation, consumption by zooplankton and bacteria). While measurements of sinking rates are very sparse for the open ocean, it is clear that they vary greatly, with observed speeds ranging from less than 1 to more than 1000 m d^{-1} (Fowler and Knauer, 1986; Asper, 1987; Asper et al., 1992; Honjo, 1996; Turner, 2002; Asper and Smith, 2003), and compilations of sinking rates are available (Diercks and Asper, 1997; Turner, 2002; Stemmann et al., 2004b).

Knowledge of the factors that control sinking rates is particularly poor. Studies with *in situ* cameras found rates varying from (<10 to several hundred m d^{-1}) and indicate a weak positive correlation of sinking rate with particle size (Asper, 1987; Diercks and Asper, 1997; Pilskaln et al., 1998; Asper and Smith, 2003), as does compilation of sinking rates determined from these and other methods (Stemmann et al., 2004b). However, for a given size, observed sinking rates vary by more than order of magnitude (Stemmann et al., 2004b). This variability is in agreement with the perspective that the biological origins and thus forms and porosities of the particles are also important (Alldredge and Gotschalk, 1988; Silver and Gowing, 1991; MacIntyre et al., 1995; Turner, 2002).

Mineral contents influence particle sinking rates and organic carbon transport. Particles collected by sediment traps moored in the deep sea exhibit correlations between organic carbon and mineral contents in both individual studies (Ittekkot et al., 1992; Ittekkot, 1993; Honjo, 1996) and global comparisons (Armstrong et al., 2002; Francois et al., 2002; Klaas and Archer, 2002), although these correlations are weaker or absent in seasonal and interannual variations at time-series sites (Dunne et al., 2005; Boyd and Trull, 2006). Whether these correlations reflect control of carbon export by mineral abundance via enhanced sinking rates (the "ballast" hypothesis), or more general influences of minerals on export such as protection of organic matter against remineralization (sometimes referred to as the "ballast ratio" hypothesis; Armstrong, 2006), or arise incidentally from relationships between ecosystem structure and carbon export is not yet clear (Ittekkot et al., 1992; Ittekkot, 1993; Honjo, 1996; Armstrong et al., 2002; Armstrong, 2006; Francois et al., 2002; Klaas and Archer, 2002). In near-surface waters, where particle organic matter contents are higher, it may be that organic matter production and aggregation controls mineral fluxes (Deuser et al., 1983; Passow et al., 1994; Passow, 2004; Passow and De La Rocha, 2006), and it is possible that organic matter control of mineral fluxes in the upper ocean grades through to mineral control of carbon flux at depth.

In this paper, we present sinking rates and mineral compositions for mesopelagic particle populations at ~300 m depth at two sites in the North Pacific, obtained with a zooplankton-excluding indented rotating sphere (IRS) sediment trap (M.L. Peterson et al., 1993) operated as an *in situ* settling column to collect fractions of sinking particles separated by their sinking rate (M.L. Peterson et al., 2005; T.D. Peterson et al., 2005). We compare our flux estimates to other trap designs used during VERTIGO, and our sinking rates to previous results from the MedFlux program in the northwest Mediterranean from bottom-moored IRS traps at ~300 m depth (Lee and Niiler, 2005; T.D. Peterson et al., 2005; Armstrong, 2006) and particles separated by sinking rate in the laboratory (Goutx et al., 2007). Finally, we offer brief speculations on the implications of varying sinking rates for carbon transport to the ocean interior.

2. Methods

2.1. VERTIGO trap deployments

We deployed the IRS sediment trap (described in detail below) at ~300 m depth beneath a free-drifting surface float (Fig. 1) for periods of approximately 1 week during the VERTIGO programs in the North Pacific. VERTIGO also examined particle fluxes at mesopelagic depths using cylindrical tube traps (0.127 m internal diameter, 0.7 m length, similar to "traditional" designs used in the HOT and BATS time-series programs (Karl et al., 1996; Michaels and Knap, 1996)). These were deployed in two ways: on rosette frames below the same surface-float mooring design as for the IRS, and on neutrally buoyant autonomous floats (Buesseler et al., 2007b).

Deployments were undertaken in oligotrophic subtropical waters in June 2004 (at station ALOHA—site of the HOT program north of Hawaii at 22.75°N, 158°W), and in mesotrophic waters of the western sub-arctic gyre in July 2005 (at the K2 time-series site operated by the Japan Agency for Marine-Earth Science Technology and collaborators, 47°N, 160°E). Overviews of the oceanographic conditions at these sites are available in companion papers (Buesseler et al., 2007b, 2008), as are particle flux results

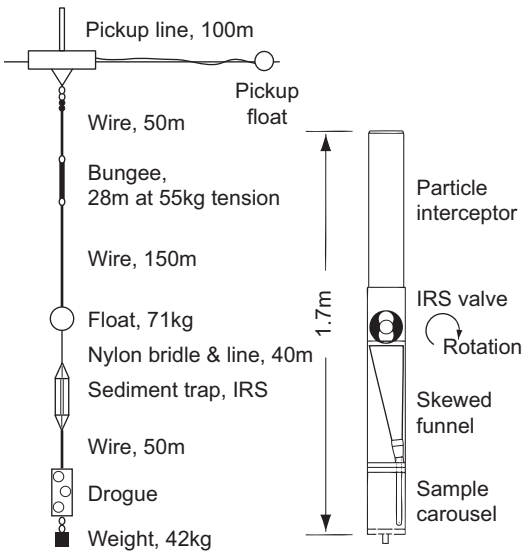

Fig. 1. IRS trap and deployment system. Key features of the IRS trap include the baffled particle interceptor tube (PIT) and the indented rotating sphere (IRS) that transfers the particles into the skewed settling funnel, for collection by 11 glass cups at the carousel (M.L. Peterson et al., 2005). The deployment system used an elastic decoupling link between the surface float and the trap to minimize vertical motion, a holey sock drogue to favor Lagrangian drift, and an Argos/GPS beacon for tracking. To minimize contamination, all bridle fittings above and below the trap were stainless steel, all wire was plastic jacketed, and the bridle and bungee were deployed directly from a plastic container to avoid deck contact. Drawing of the IRS trap modified from M.L. Peterson et al. (2005).

from moored sediment traps (Honda et al., 2006), the VERTIGO surface-suspended and neutrally buoyant traps (Buesseler et al., 2008; Lamborg et al., 2008), and studies of food-web structure (Boyd et al., 2008; Steinberg et al., 2008b).

2.2. Collection of particles separated by sinking velocity

The trap has been described previously (M.L. Peterson et al., 1993, 2005; T.D. Peterson et al., 2005), and was built to order by Prime Focus, Inc. (Seattle, WA, USA). The particles are collected into a ~0.8 m long, 0.152 m internal diameter cylindrical "particle interceptor" tube (slightly larger but of similar aspect ratio to the other VERTIGO traps which were 0.7 m long, with 0.127 m internal diameter). The tube was fitted at the top with a baffle with 0.015 m rectangular openings to exclude fish (the other VERTIGO traps had a similar baffle with ~0.01 m hexagonal openings). The IRS fits tightly at the base of this tube and when rotated transfers the particles to a skewed funnel that provides a clear vertical path to the carousel of 12 collection cups below.

In sinking-velocity mode, the carousel is rotated through all carousel positions each time that the IRS is rotated. This separates the particles according to the time required to settle from the IRS to the carousel below. This settling distance is not particularly well defined since particles can depart from the IRS surface at any point between tangentially at the edge of the IRS (a distance of 0.64 m for our trap), or radially from the bottom of the IRS (a distance of 0.57 m). We have used the shorter distance in our calculations since this ensures that the stated velocities are minima. Other IRS trap studies have reported a slightly longer settling length of 0.68 m (Lee and Niiler, 2005; T.D. Peterson et al., 2005; Armstrong, 2006). Eleven positions collect samples into 100-mL glass cups, the 12th is an open hole used during deployment and recovery. The sample cups were filled with poisoned brine (salinity ~50 g L^{-1}, $HgCl_2$ 150 mg L^{-1}, filtered through a ~0.8 mm GF/F filter) to retard loss during carousel movements and bacterial activity.

We programmed the IRS to rotate every six hours, and the carousel to separate the particles into sinking velocities fractions decreasing from >820 to 2 m d^{-1} (Table 1). This is a more rapid IRS rotation cycle than the 24 h used in previous deployments of IRS traps in sinking-velocity mode as carried out during the MedFlux program in 2003 and 2005 (M.L. Peterson et al., 2005; Lee and Niiler, 2005; Armstrong, 2006). This shorter cycle was motivated by the desire to minimize particle–particle interaction and zooplankton grazing on the upper surface of the IRS. The particles will of course continue to remineralize during their repose on the IRS. If the particles arrive steadily in time, the ratio of the incoming flux to the remineralized flux that is transferred to the carousel can be written (Lamborg et al., 2008):

$$R_F = \frac{kt}{1 - e^{-kt}},$$

in which k is the first-order remineralization constant and t is the IRS rotation duration of 6 h. Even remineralization rates as high as 0.8 d^{-1} lead to a reduction in flux of less than 10% (much higher than the value of ~0.25 d^{-1} required to reproduce the flux attenuation with depth at K2 from the sinking rates reported here—see Section 4). Thus, this effect is negligible in comparison to other uncertainties in the estimation of absolute fluxes from traps (Gardner, 2000; Buesseler et al., 2007a), and in comparison to variations among individual traps during VERTIGO of ~30% (Lamborg et al., 2008). Similar considerations hold for the abiotic dissolution of particles once they enter the poisoned brine, and based on DOC release rates during VERTIGO deckboard incubations of recovered particles these effects are even smaller and can also be ignored (Lamborg et al., 2008), although they must be accounted for in longer term moored trap studies (Antia, 2005). The longer IRS rotation period of 24 h used during the MedFlux studies might have reduced those fluxes to a greater extent, but how this would have affected the flux variations as a function of sinking rate is not known.

Table 1
Trap cup rotation schedule and sinking rates

Cup #	Open (h:min)	Close (h:min)	Duration (min)	Sinking rate (m d^{-1})
1	0:00	0:01	1	>820
2	0:01	0:02	1	410
3	0:02	0:04	2	205
4	0:04	0:06	2	137
5	0:06	0:08	2	102
6	0:08	0:16	8	51
7	0:16	0:32	16	26
8	0:32	1:04	32	13
9	1:04	2:08	64	6
10	2:08	5:59	231	2.3
11	5:59	6:00	1	2.3, "blank"
12	Open hole			

1. Cup rotation times are with respect to the most recent IRS rotation.
2. The sinking rates are the minimum value to enter each cup.
3. Vertical settling distance from IRS to cup was 0.57 m.
4. Cup 11 collected material sinking at 2 m d^{-1} for 1 min, as a check on "carry-over" to the next cycle and the processing blank—see text.

Using the 6-h cycle limits the minimum sinking rate that can be investigated to ~2 m d^{-1} (versus 0.68 m d^{-1} with the 24 h cycle and slightly longer fall distance in the MedFlux studies), and also increases the risk that particles settling slower than this minimum may remain in the funnel through an entire cycle and be collected in a subsequent cycle. To control for this possible problem, we programmed the last cup (#11) to reside beneath the funnel for 1 min (Table 1), so that the flux it collects provides an estimate of the possible contribution of slowly sinking particles to the subsequent collection of fast-sinking particles after the next IRS rotation (for which the cup opening duration is also 1 min).

We deployed the IRS trap inside a cylindrical cage suspended by a three-part bridle below a free-drifting surface float via an elastic link that decouples the trap from surface motions (Fig. 1). For the most part, our design maintained the target depth to within a few meters as recorded by an onboard pressure sensor (Fig. 2). However, the relatively low sensor temporal resolution of 2 min and depth resolution of ~3 m cannot rule out surface wave or higher frequency motions. Thus, we cannot directly address the possibility that these may have affected the particle collection, other than to note that VERTIGO flux results from other surface-tethered traps were similar to those from subsurface neutrally buoyant traps (Lamborg et al., 2008). The surface float was equipped with an Argos/Global Positioning System beacon and a coded strobe light to aid recovery, and to distinguish it from the multitude of other drifters released during the VERTIGO missions. At both the ALOHA and K2 sites, the drift tracks of the IRS trap (Table 2) were very similar to those of the surface-suspended and neutrally buoyant sediment traps (NBSTs) deployed at the same time (Buesseler et al., 2008), suggesting that hydrodynamic biases on trap collection were minimal or at least similar (Gardner, 2000; Buesseler et al., 2006). Two IRS trap deployments were undertaken at each site, but the first deployment at ALOHA failed owing to an error in the on-processor code as supplied by the manufacturer.

In addition to the deployments, we briefly examined the functioning of the IRS trap in a shipboard laboratory during the ALOHA mission. We filled the system with filtered seawater and released ~100 particles (collected with a McLane PARFLUX conical

Table 2
Trap deployments

Site name	Depth (m)	Duration (d)	Drift (km)	Deployment action	Longitude (°W)	Latitude (°N)	Date (dd/mm/yyyy)	Time (hh:mm)
ALOHA-2	272±3	6.5	45	Launch	157.998	22.750	02/07/2004	10:00
				Retrieve	157.878	23.141	08/07/2004	22:00
K2-1	285±4	6.5	35	Launch	−160.997	46.999	30/07/2005	07:00
				Retrieve	−161.448	47.055	05/08/2005	19:00
K2-2	281±4	6.5	22	Launch	−161.001	47.000	10/08/2005	07:00
				Retrieve	−161.239	47.116	16/08/2005	19:00

1. All times are UTC, ALOHA local time was UTC−10 h, K2 local time was UTC+11 h.
2. Depths are means ±1 S.D. from a Vemco pressure logger mounted on the trap.
3. Drift distance is between start and end points, not along path.
4. Dates/times are for collection period; positions are for launch and retrieval.

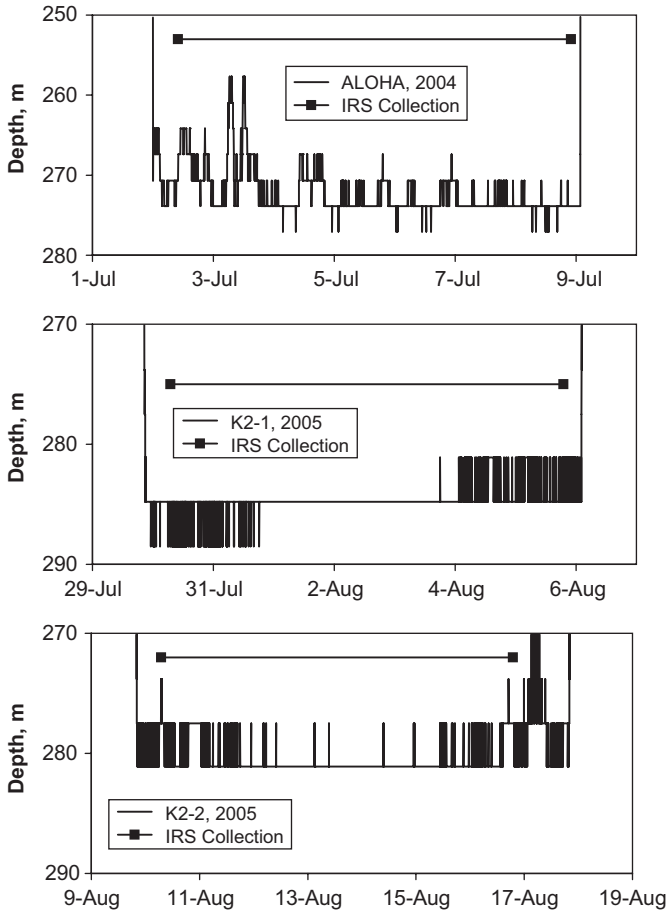

Fig. 2. Records of IRS trap depth for the ALOHA and K2 deployments. The trap collection periods are marked by horizontal bars. The ALOHA record shows significant variations early in the deployment, and then more quiescent conditions. For most of the K2 deployment periods the depths were constant, showing either no variations or single-bit noise at the relatively poor depth resolution of the sensor (~3 m). The K2-2 deployment experienced bad weather (~35 knot winds) just after the end of the collection period, which dragged the trap to shallower depths, and delayed trap recovery until the weather eased.

sediment trap at 300 m depth) into the IRS particle interceptor tube and watched the delivery of these particles via the IRS and skewed funnel into the carousel collection cups. Within the limitations of our observations, which focused on the larger particles (~0.3 to 3 mm), the trap performed essentially as expected. Almost all particles were released within the first 20–30° of rotation from the horizontal, with only one particle observed to remain on the surface of the IRS beyond 90° to be released at ~120°. This ready release may reflect the particle types and/or the highly polished surface of the IRS as received and maintained. No particles were observed to be released above the IRS within the particle interceptor tube during the rotation. This result may reflect the relatively large size of the particles, and/or the dimple pattern of the IRS, which consisted of concentric rings about the vertical axis, with a ridge at right angles to this pattern (the pattern is depicted in Fig. 3C of T.D. Peterson et al., 2005). This ridge is co-axial to the rotation axis and serves to ensure a smooth fit of the IRS to the particle interceptor tube throughout the rotation. Further discussion of the operation of the IRS trap and associated possible biases in sinking rates is available in T.D. Peterson et al. (2005).

2.3. Chemical analyses

On recovery, each IRS trap sample cup was quantitatively transferred to a vacuum filtration funnel using filtered seawater (0.8 μm) for rinsing, and filtered onto a 25-mm diameter 1.2-μm pore silver membrane filter (Sterlitech, Kent, WA, USA). The filters were then photographed at magnification 6.5–50 × and dried at 50 °C, and divided into quarters for chemical analyses. Total particulate carbon (PC) and nitrogen (PN) was analyzed by high temperature combustion against acetanilide standards on a Thermo Electron Flash Elemental Analyser Model 1112. Particulate inorganic carbon (PIC) was analyzed by closed-system acid digestion and coulometric CO_2 titration following Honjo et al. (2000). Biogenic silica was analyzed by sodium hydroxide digestion and spectrophotometry using an Alpkem autoanalyser following Queguiner (2001). For each of these three analyses, 1/4 of the filter was used. The fourth quarter was used to attempt stable isotope analyses with limited success (not reported here). No filtering blank correction was made for any analyte, based on the filter photographs and results from filtrations of the cup brines prior to deployment that yielded negligible PC contents (<1% of any sample).

POC was calculated as PC–PIC. For the ALOHA samples, the PIC analyses were not undertaken because the sample amounts were very small, and we report only PC values (with estimates for POC based on PIC/PC ratios from other VERTIGO traps). Each of these analytical methods had precisions of a few percent, but the overall precision was controlled by the division of the sample into quarters. Based on the inhomogeneity of coverage of the filter surface as seen in the photomicrographs (Fig. 3), and (unpublished) experience with replicate POC analyses of similar filters, we estimated that this precision would be on the order of 30%, but

could have been as high as a factor of 2 or more for those fractions for which a few large particles appeared to dominate the sample. Without sufficient material to allow homogenization nor replication, this error was unavoidable and remains poorly constrained. Thus, we are unable to provide individual uncertainty estimates for individual fractions. Therefore, in the discussion below, we allow for the possibility that this sub-sampling has biased the distribution of sinking rates as well as the ratios of the chemical components. Future studies may benefit from combining sinking-rate fractions to allow replication of analyses, at the expense of lower resolution of the flux as a function of sinking rate.

3. Results

3.1. Total fluxes

The ALOHA-2 total PC flux (summed over all sinking-rate fractions; Table 3) of 283 μmol m^{-2} d^{-1} for the IRS trap was considerably lower than the flux of 700 $\pm$ 180 μmol m^{-2} d^{-1} obtained by averaging PC results from two neutrally buoyant traps and a single surface-suspended trap deployed at similar depth (300 m) for shorter but overlapping periods during VERTIGO (Lamborg et al., 2008). At K2, where POC fluxes were measured, this comparison shows that the IRS trap total POC fluxes were also lower than POC flux results from the other three VERTIGO traps for the first K2-1 deployments (830 μmol m^{-2} d^{-1} for the IRS trap vs. 3350 $\pm$ 960 μmol m^{-2} d^{-1} for the other traps), but that all traps obtained similar results for the second K2-2 deployments (1411 μmol m^{-2} d^{-1} for the IRS trap vs. 1500 $\pm$ 300 μmol m^{-2} d^{-1} for the other traps). It is possible that the flux variations between the IRS and other VERTIGO traps stem from real small-scale spatial variability, given the small number of particles collected by the IRS trap in its single particle interceptor tube. For the other VERTIGO traps, multiple tubes were combined (two pairs of two individual tubes from each neutrally buoyant trap and each surface-suspended trap) to obtain those flux results (Lamborg et al., 2008). Thus, the standard deviations from replicate arrays of the VERTIGO neutrally buoyant and surface-suspended traps of ~30% (Lamborg et al., 2008), may underestimate the small scale variability by a factor of ~2 (i.e., the square-root of the number of combined tubes), so that the IRS trap results are close to indistinguishable from the other traps results.

Alternatively, the IRS system may cause lower fluxes, e.g., if zooplankton feed on the particles during its residence on the upper surface of the IRS (although bacterial remineralization during this period can be neglected—see Section 2.2), or if movement of the trap or IRS resuspends particles and prevents their transfer to the trap interior. Differences in the amount of zooplankton entering the traps may have played a role as well, although zooplankton were removed from the VERTIGO neutrally buoyant and surface-suspended traps (amounting to ~10–15% of the total POC flux at ALOHA and ~50% of at K2 for traps at 300 m depth (Lamborg et al., 2008). Although this removal does not address a possible contribution from fecal pellets from these animals (Noji et al., 1991).

3.2. Effectiveness of the separation of particles by their sinking rates

The results for the individual cups from each IRS trap deployment are shown in Table 3. We focus first on the POC fluxes. POC was measured for all the K2 samples (as the difference PC–PIC). For the ALOHA samples, PIC was not measured and we use the approximation POC $\approx$ PC, based on the POC/PIC ratios of 5–10 observed in other VERTIGO traps at ALOHA at 300 m depth (Lamborg et al., 2008). The cups from each deployment were processed somewhat differently on recovery and this affects our interpretations. At ALOHA, the visually small amounts of material in all the collection cups led us to combine several cups. Microscopic inspection of these filters did not reveal any obvious signs of zooplankton that might have entered the trap by swimming, and therefore we did not undertake any further processing. At K2, we did not combine any cups, but for the first deployment (K2-1) we did remove large ($>$1 mm) radiolarian zooplankton from the filters, and analyzed their PC contents separately (as shown in parentheses in Table 3). These animals are not active swimmers but may migrate in the water column and may have entered the trap alive. For the second deployment (K2-2), we did not remove these organisms, and they were analyzed on the filters as part of the flux (a decision we now regret, but which seemed sensible while at sea, following debate as to whether these animals were alive or dead, swimming or sinking).

The first issue to resolve from the observed PC flux variations among the collection cups is whether the IRS trap functioned appropriately to separate particles by their sinking rates. Programming the last cup (#11) to remain open for just one minute was central to this assessment and we recommend that this approach be adopted in all future applications of the IRS trap in sinking-velocity mode (to our knowledge it has not been used previously). Our expectation was that this cup would collect very little material, thereby indicating that all particles had settled from the funnel prior to the delivery of new particles from the next IRS rotation. If a significant amount of the particles were still settling, then we expected that this last cup would collect a similar amount to the previous cup, when scaled to their relative duration of opening (i.e., fluxes in the ratio (1/231 min) for cups #11/#10; Table 3).

To our surprise, cup #11 collected a significant amount of material during all three deployments, and in terms of flux per unit duration that the cup was open (F_{pcd}; Table 3), cup #11 collected more material than the preceding cup #10. For the ALOHA deployment, the F_{pcd} for cup #11 was 50 times higher than for cup #10, and for the K2 deployments this statistic reached several hundred. How might this occur? We have been able to think of only one possible explanation—material that settles slowly in the funnel is for some reason delivered preferentially to cup #11. The longest period available for material to settle is during the time when cup #10 is open (~2/3 of the total 360 min cycle). It may be that material sinks to the entry of the carousel during this time but is not transferred to a cup until the carousel rotates. This could occur if the sinking material agglomerates in some way that prevents it passing into the cup until the movement of the carousel occurs. We used brine within the cups and its increased density may have been sufficient to prevent entry of slow-sinking particles (with little excess density above that of seawater), so that they remained at the interface between the cup and the funnel until the movement of the carousel pushed them into the subsequent cup. The timescale for the brine to penetrate particle interstices depends strongly on particle permeability, with estimates for mm-sized highly porous flocs and marine snow of the order of 10^2–10^4 s (MacIntyre et al., 1995); i.e., sufficiently slowly that larger or less permeable particles such as the cm-scale phaeodarians recovered from these cups (see the photographs in Fig. 3) could have been retarded by the brine for timescales of the IRS rotation period. The brine was used to minimize the possibility of loss of poison from the cups during their exposure to the funnel, and for comparability to other VERTIGO traps which also used brine. In hindsight, an alternate system of maintaining poison levels without brine, such as the inclusion of poison "diffuser" vials within the cups (M.L. Peterson et al., 2005) would have been a better choice.

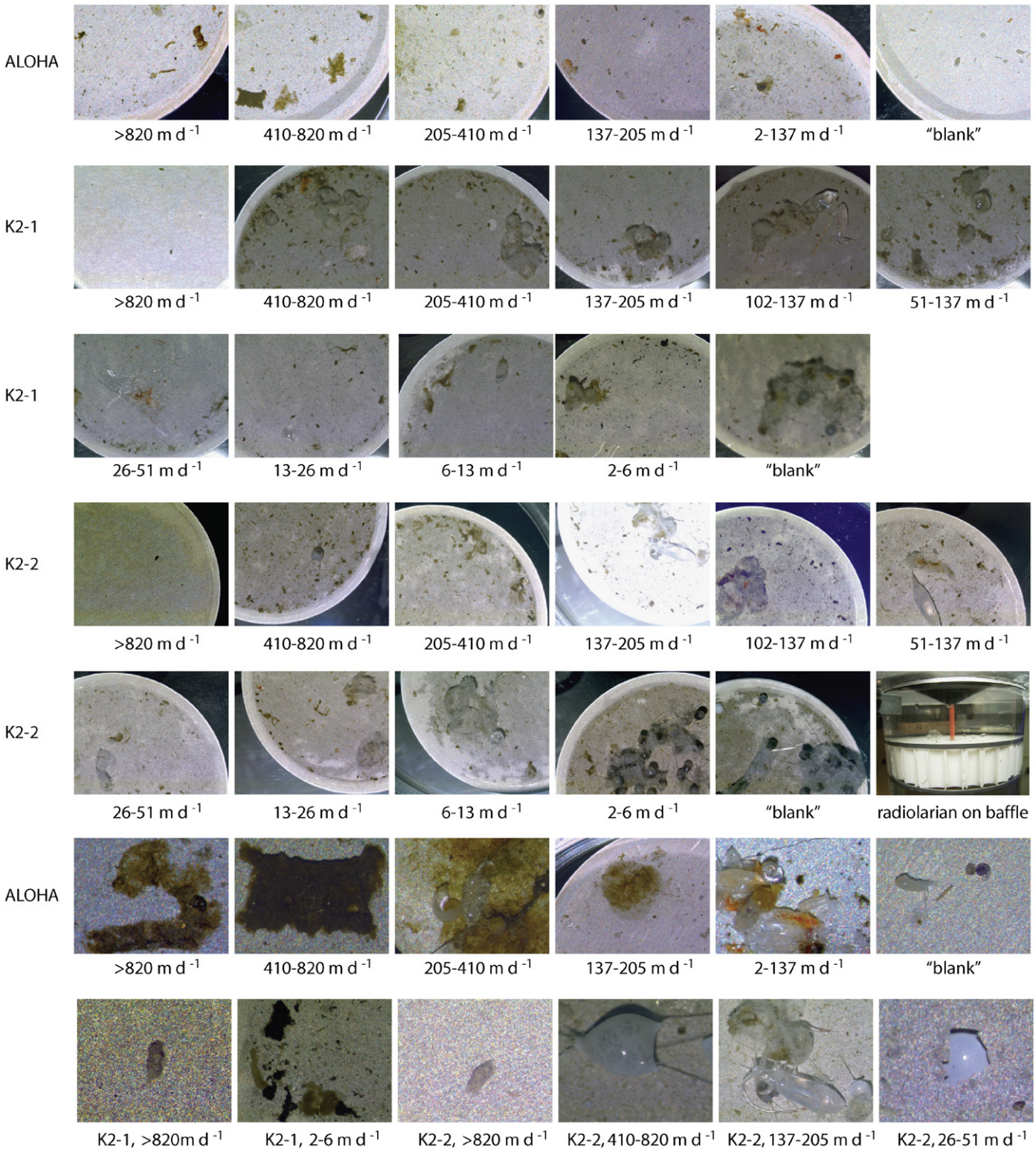

Fig. 3. Photos of IRS trap particles after filtration onto 25-mm diameter silver filters. The general character of the particles is shown by overview images at 6.5 × of ~1/4 of each filter (top five rows). Details of particle types are shown by close-up images at 50 × (bottom two rows). ALOHA: the overview images reveal that very large (mm) fecal pellets were common in the fast-sinking fractions (>820, 410, 205, 137 m d^{-1}), with more fluffy aggregates and smaller fecal pellets observed in the combined slowest-sinking fraction (2–137 m d^{-1}). Low particle abundances were observed in the cup #11, 1 min duration, "blank" sample, although not when scaled in terms of POC flux per unit time (see text for discussion). Close-up images revealed gastropod and foraminifera shells in the fast-sinking fractions, and copepod carapaces in the combined slowest-sinking fraction. Whether the association of shells with fecal pellets (e.g., as shown in the close-up of the >820 m d^{-1} fraction) formed in the ocean or during filtration is unknown. K2: the overview and close-up images of the fastest sinking fraction (>820 m d^{-1}) for both deployments reveal extremely low flux, consisting of a few dense pellets that appeared to have black spiky materials within them. Other fractions tended to be dominated by fecal pellets derived (Wilson et al., 2008) from the abundant copepods observed in net-hauls (Steinberg et al., 2008b) and radiolarian zooplankton (often clumped together, presumably during filtration). The slowest-sinking fraction during the K2-1 deployment (2 m d^{-1}) differed from this generalization in having a large amount of a black, low density, organic membrane-like material that fragmented on the filter). The cup #11 "blank" samples were dominated by the presence of a single phaeodarian zooplankton for both K2 deployments. This organism was removed and analyzed separately for the K2-1 deployment, but analyzed on the filter for the K2-2 deployment—see text for discussion. A photo of a very large organism of this type is also shown, as recovered in a separate VERTIGO deployment of a surface-tethered cylindrical sediment trap.

Table 3
Trap fluxes and compositions

Deployment	Cup #	Sinking rate fraction ($m\,d^{-1}$)	Cup duration per cycle (min)	POC flux per cup ($\mu mol\,m^{-2}\,d^{-1}$)	POC flux per cup duration ($\mu mol\,m^{-2}\,d^{-1}\,min^{-1}$)	POC flux fraction ‘	POC flux cumulative fraction (%)	POC/PN ratio (mol/mol)	POC/PIC ratio (mol/mol)	POC/Bsi ratio (mol/mol)
ALOHA-2	1	820	1	44	44	16	16	nd	nd	33
	2	410	1	31	31	11	27	nd	nd	2
	3	205	2	27	14	10	36	nd	nd	Bsi bd
	4	137	2	25	12	9	45	nd	nd	1
	5	102	2	*These cups combined with cup 10*						
	6	51	8							
	7	26	16							
	8	13	32							
	9	6	64							
	10	2	231	126	0.5	45	89	nd	nd	62
	11	“blank”	1	30	30	11	100	nd	nd	3
		Sum	360	283		100		nd	nd	5
K2-1	1	820	1	bd	bd	bd	bd	Both bd	POC bd	Both bd
	2	410	1	271	271	33	33	10	9	1
	3	205	2	102	51	12	45	10	4	0.4
	4	137	2	110 (15)	55	13	58	10	9	1
	5	102	2	87 (42)	43	10	69	9	4	1
	6	51	8	71 (20)	9	9	77	10	3	0.3
	7	26	16	64	4	8	85	11	5	9
	8	13	32	23	0.7	3	88	PN bd	2	1
	9	6	64	41	0.6	5	93	11	2	1
	10	2	231	31	0.1	4	96	9	2	3
	11	“blank”	1	30 (472)	30	4	100	16	5	2
		Sum	360	830 (549)		100		10	4	1
K2-2	1	820	1	bd	bd	bd	bd	Both bd	POC bd	Both bd
	2	410	1	109	109	8	8	13	8	0
	3	205	2	82	41	6	14	14	6	1
	4	137	2	346	173	25	38	13	24	3
	5	102	2	92	46	7	45	10	8	2
	6	51	8	191	24	14	58	7	15	3
	7	26	16	67	4	5	63	8	15	3
	8	13	32	60	1.9	4	67	10	7	1
	9	6	64	65	1.0	5	72	8	4	2
	10	2	231	399	1.7	28	100	6	PIC bd	4
	11	“blank”	1	0 (576)	576	*Set to 0*		6	5	10
		Sum	360	1411 (576)		*100*				

1. The POC flux per duration, is the POC flux divided by the cup opening duration, referred to for simplicity as ‘Fpcd’ in the text.
2. K2-1 POC flux values in parentheses are the POC contents of zooplankton removed from the samples and analyzed separately, expressed in units of flux. Zooplankton were not removed from the ALOHA or K2-2 samples—see text for discussion.
3. nd—not determined, bd—below detection.
4. For the K2-2 cup #11, the fractional POC flux was 46%, but was set to 0% to calculate the cumulative distribution function because the cup contents were dominated by a large zooplankon similar to the organism that dominated but was removed from the K2-1 cup #11—see text for discussion.
5. For ALOHA only, all POC values are actually PC values, as PIC was not measured—see text for estimates of PIC based on other trap results at ALOHA.

The photographs of the materials as collected on the filters lend support to the hypothesis that slow-sinking materials were preferentially delivered into cup #11. For both deployments at K2, cup #11 contained a very large (~1 cm) phaeodarian (colonial radiolarian). This zooplankton consists of a nearly transparent spheroidal net-like structure decorated externally with large blebs of dark material (Fig. 3). It remained remarkably intact and was easily lifted from the filter with forceps. For deployment K2-1, for which large zooplankton were removed from the filter and analyzed separately, this single zooplankton completely dominated the carbon content of cup #11 (supplying POC equivalent to a flux of 472 $\mu mol\,m^{-2}\,d^{-1}$ in comparison to 30 $\mu mol\,m^{-2}\,d^{-1}$ for all other material on the filter; Table 3). Separate analysis was not carried out for deployment K2-2, but the photographs tell the same story—a large phaeodarian dominates the material on the cup #11 filter. We believe that this result must reflect arrival of this large organism to the carousel opening during the cup #10 long opening duration, followed by its transfer to cup #11 when the carousel moves, as the probability of this organism arriving during the 1 min opening duration of cup #11 in both deployments would seem to be very small.

It does not appear that the carry-over at K2 of slow-sinking material from the cup #10 collection period into cup #11 continued on to the successive cup #1 of the next IRS rotation cycle. The K2 cup #1 filters exhibited no large particles; in fact they were virtually free of particles except for (in both cases) two small dense pellets that appeared to contain spiky black fragments (Fig. 3). The low F_{pcd} (flux per cup opening duration) values for the K2 cup #1 collections (in comparison to corresponding cup #11 values; Table 3) also support the view that whatever the process that enhanced the cup #11 collections, it did not affect the subsequent IRS rotation cycle. It may be that the passage over the open hole between cup #11 and cup #1 acts to clear any remaining material at the carousel mouth—e.g., via a flow of fluid out the bottom of the system. A reasonable maximum estimate for the carry-over is the total POC content of cup #1, which was negligible in comparison to subsequent cups for both K2 deployments.

3.3. The variation of flux as a function of sinking rate

As discussed in the previous section, while the trap does appear to have separated particles by their sinking rates, this separation was not ideal. Large slowly sinking material, in particular phaeodarian zooplankton at K2, may have been collected at the time of carousel rotation from cups #10 to #11 rather than at the time of their arrival. This has little impact on their calculated sinking rate since those cups collected particles sinking at 2–6 and 2.3–2.4 m d^{-1}, respectively. However, how we choose to treat the collection of these organisms does strongly affect our view of the variation of flux as a function of sinking rate. If we treat the contribution from these large organisms as part of the flux, then the sum of these two slow-sinking fractions (#10 and #11) represents approximately one-third of the total POC flux for both K2 deployments. Considering the possibility of loss of slow-sinking material as the carousel rotates across the open hole would further increase the influence of slow-sinking material on the total flux.

In contrast, if we consider that the phaeodarians were living organisms and thus appropriately removed from the filters and from the estimation of sinking flux, then our view changes considerably. In the K2-1 deployment, this leads to a view of the POC flux distribution that emphasizes fast-sinking particles, with only ~8% of the PC flux sinking slower than 6 m d^{-1} (as collected in cups #10 and #11; Table 3). A similar conclusion is obtained for K2-2 to the extent that much of the material in the two slowest-sinking fractions (cups #10 and 11) consisted of phaeodarian and other radiolarian zooplankton as seen in the photographs (Fig. 3). However at ALOHA, while the photographs reveal a wide diversity of particle types there is no indication that the slowly sinking fractions consisted of extant zooplankton to a greater degree than in the other cups.

Whatever interpretation is chosen for the slow-sinking fractions, it is clear that fast-sinking particles were present at K2 and ALOHA. For the K2-1 deployment, after removal of the zooplankton swimmers, particles sinking at >102 m d^{-1} made up 69% of the POC flux (Table 3). For the K2-2 deployment, this fraction made up 45% of the POC flux (if cup #11 is ignored based on the photographic evidence that it was dominated by a large phaeodarian). At ALOHA, 38% of the POC flux was in the fractions sinking at >137 m d^{-1}, but the single deployment and small amounts of material collected emphasize that this result must be viewed with caution.

3.4. Compositional variations among sinking-rate fractions

The POC/PN ratios for the total fluxes (summed over the fractions) at K2 were 8–10 (Table 3), somewhat above the canonical Redfield phytoplankton value of 6.6, but similar to results from the VERTIGO neutrally buoyant and surface-suspended traps (Lamborg et al., 2008). There were no clear variations with sinking rate for the K2-1 deployment, but the K2-2 deployment showed a decrease in POC/PN ratio from values of ~13 for rapid sinking particles to values of ~8 for slower sinking particles. There was no change in bulk POC/PN ratios between deployments 1 and 2 for the VERTIGO neutrally buoyant and surface-suspended traps (Lamborg et al., 2008), so that this change with sinking rate is unlikely to be an alias of a change in the character of the sinking particles over time. A possible interpretation is a transition from N-poor fecal pellets in fast-sinking fractions towards more N-rich phytoplankton aggregates in slower sinking particles. POC/PN ratios were not obtained for our ALOHA samples (as we did not measure PIC), but were presumably similar to those obtained from the neutrally buoyant and surface-suspended traps during VERTIGO of ~8.5 (Lamborg et al., 2008).

The IRS POC/PIC ratios for the total fluxes were 4 for K2-1 (after zooplankton removal) and 17 for K2-2 (without zooplankton removal), which can be compared to results for total fluxes from the other VERTIGO traps of ~8 for K2-1 and ~25 for K2-2 (Lamborg et al., 2008), and estimates of ~10 for global fluxes from the surface ocean (Yamanaka and Tajika, 1996; Koeve, 2002). The K2-1 deployment showed a weak trend of decreasing POC/PIC with decreasing sinking rate (Table 3), the opposite to that which would be expected if PIC acted to increase sinking rates. No clear trend was discernable in the K2-2 deployment. However, the >820 m d^{-1} fractions for both K2-1 and K2-2 contained significant PIC (equivalent to PIC fluxes of 25 and 23 μmol m^2 d^{-1}, respectively), although both POC and BSi below detection for these samples (Table 3). PIC was not measured for our ALOHA samples, but results from the VERTIGO NBST and surface-suspended traps at 300 m depth at ALOHA indicate a POC/PIC ratio of 5–10 (Lamborg et al., 2008). Unsurprisingly, all of the VERTIGO observations of POC/PIC ratios were much higher than values of less than 1 that characterize deep-ocean sediment trap materials (Armstrong et al., 2002; Klaas and Archer, 2002; Boyd and Trull, 2006), emphasizing the difference between organic matter dominated mesopelagic particles and mineral dominated deep ocean particles.

The POC/BSi ratio at K2 was close to 1 for the total summed fluxes, with a maximum value of ~10 for the individual fractions (Table 3). This emphasizes the importance of diatoms to the sinking flux. No trend in POC/BSi with sinking rate was discernable for either the K2-1 or K2-2 deployments. At ALOHA, PIC was not measured, but based on the VERTIGO results of POC/PIC of ~5–10 at 300 m depth (Lamborg et al., 2008) our measured PC/BSi ratios were probably dominated by POC. These varied widely from 1 to 63, but with no clear dependence on sinking rate.

4. Discussion

It is clear that the IRS trap is not a perfect tool for the determination of *in situ* particle sinking rates. It is a technology undergoing active refinement. The modified cup programming sequence presented here offers an advance in the evaluation of the sinking-rate separation process, although it raised nearly as many questions as it answered. Another useful technique might be to release calibration particles such as colored glass spheres, fluorescent plastic beads, or sieved organic particles such as walnut shells into the particle interceptor tube during a test deployment, as has been done for other trap designs (Gust et al., 1996; Buesseler et al., 2007a). Other recently proposed improvements include the addition of cameras to track particle motions in both the particle interceptor tube and the settling funnel, and a pump to periodically clear the funnel through a collection filter (T.D. Peterson et al., 2005). The short IRS rotation cycle during VERTIGO allowed individual particles to be photographed in detail (albeit after filtration). Further improvement in the recovery of morphometric information might be achievable by using polyacrylamide gel within the IRS trap cups to gently decelerate and isolate particles (Lundsgaard, 1995; Ebersbach and Trull, 2008), although questions about particle alteration on the surface of the IRS and within the funnel would still remain.

The short deployment periods that allowed us to photograph separated particles offer some important insights to both trap functioning and the control of export flux. First of all, very few zooplankton active "swimmers" were collected. This is in strong contrast to the considerable abundance of copepods collected at 300 m in the VERTIGO neutrally buoyant and surface-suspended

traps, in which zooplankton contributed ~50% of the total POC collected at K2 and ~15% at ALOHA (Lamborg et al., 2008). Thus, the IRS trap functioned very well to meet its original design goal of excluding "swimmers" (M.L. Peterson et al., 1993). However, non-swimming zooplankton ("surfers") were collected by the IRS trap (as they have been in previous neutrally buoyant sediment trap deployments; Buesseler et al., 2000) and these organisms (especially the radiolarians and phaeodarians at K2) represented an important confounding factor in the estimation of sinking particle fluxes. Second, the photos reveal a wide range of particle types within each sinking-rate fraction. This suggests that the biological origins and forms of particles are influential. In particular, particle porosity, or in other words the tightness of particle packing, is an important consideration, as has been emphasized from laboratory and field studies of fecal pellets, aggregates and aggregation processes (Alldredge and Gotschalk, 1988; Jackson, 1995; Alldredge, 1998; Turner, 2002; Stemmann et al., 2004b). This effect may contribute to masking the role of density increases from the incorporation of biogenic minerals, and thus partly explain the lack of a clear correlation between sinking rates and particle PIC or BSi contents in our observations, or those obtained during MedFlux (Lee and Niiler, 2005). Moreover, the bulk chemical analyses used here and elsewhere to assess the role of biogenic minerals does not address variations in the forms and origins of these materials or resolve specific associations with POC for individual particles.

As noted in Section 1, in addition to the basic goal of obtaining *in situ* sinking rates for mesopelagic particles, a longer term objective of this work is to investigate the possibility that mesopelagic particle sinking rates vary significantly among ocean ecosystems. As a first step towards this goal, Fig. 4 compares the POC fluxes as a function of sinking rate for all the VERTIGO deployments, as well as two MedFlux deployments from similar depth (~300 m) in the northwest Mediterranean. The MedFlux results displayed very similar distributions for two different deployment years (2003 and 2005), which can be reasonably approximated as Gaussian distributions with means of ~350 m d^{-1}, with an additional exponential tail of slow-sinking particles (Armstrong, 2006; Lee and Niiler, 2005). An important role for fast-sinking particles in the total POC flux also was suggested by the significant fraction sinking faster than 230 m d^{-1} in laboratory experiments using particles collected from the MedFlux site (Goutx et al., 2007). The VERTIGO ALOHA results are indistinguishable from the MedFlux results, especially given the limited number of sinking-rate fractions that could be determined at ALOHA, and that this comparison requires the unjustified assumption that the POC/PIC ratio of all ALOHA sinking-rate fractions was similar (as only PC was measured for ALOHA). The K2-2 results are also similar to the MedFlux results. This is readily apparent in Fig. 4 for the mid-range of sinking rates, and also true for slower sinking rates when lower resolution of the slowest-sinking-rate fractions during VERTIGO than MedFlux is taken into account).

The only distribution that stands out is the K2-1 result. But it is not clear as to whether this represents a truly different spectrum of sinking rates, or simply the influence of what material is included in the flux estimates. First of all, our 6-h IRS rotation schedule may have missed some of the slow-sinking particles, which could explain some of the difference. Second, the K2-1 results are the samples from which non-motile zooplankton were removed and not counted as part of the flux. In particular, we discounted the large amount of very slow-sinking material in the slowest-sinking fraction (cup #11; Table 3). If we included this material it would push the K2-2 curve down closer to the other distributions. This emphasizes one of the most important results of our study—that the role of non-motile zooplankton in the

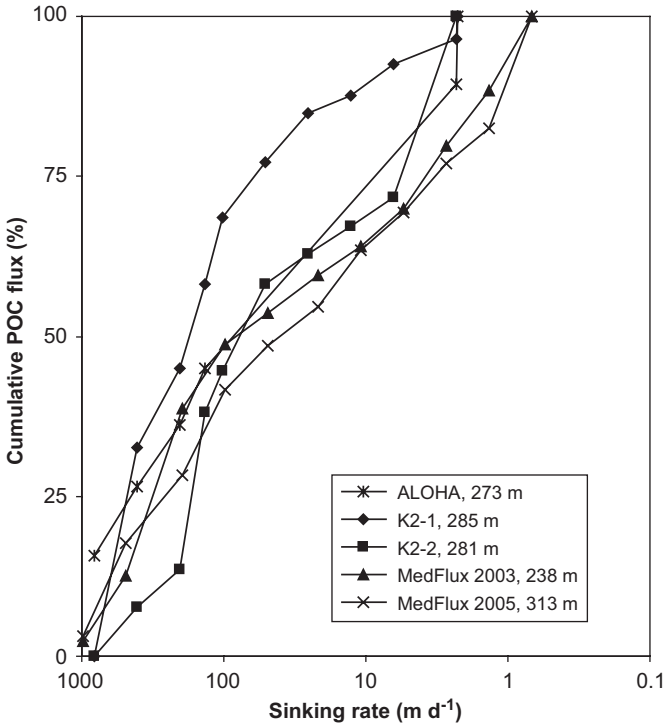

Fig. 4. Cumulative distribution functions for particulate carbon (POC) flux as a function of sinking rate. The VERTIGO K2 results are those after subtraction of non-motile zooplankton POC (see Table 3). The MedFlux results are for a site in the northwest Mediterranean using a longer IRS rotation cycle of 24 h (M.L. Peterson et al., 2005; Lee and Niiler, 2005) that allowed resolution down to slower sinking rates (0.68 m d^{-1}).

assessment of sinking particle fluxes requires careful attention at mesopelagic depths. Our short-term deployments allowed us to make some estimate of their contribution, but the extent to which this was possible during MedFlux is less clear (as these organisms if present may have disintegrated sufficiently during those longer deployments to be considered as part of the flux). Thus, the differences may reflect differences in the material counted as part of the flux. Given these uncertainties and the un-replicated nature of our observations, we do not present a statistical evaluation of the variations among the cumulative distribution functions.

Overall, the similarity of our observations to previous results are in support of the suggestion that the distribution of particle sinking rates may evolve towards a characteristic shape relatively independently of particle composition (Armstrong, 2006). More observations are needed to test this idea (especially via multiple techniques to verify that these sinking-rate distributions are real properties of the marine particles and are not driven by the IRS trap collection process) and perhaps also new conceptual models for sinking particle interactions. It is unlikely that these models will escape the need to consider food-web structures and other biological processes, but the similarity of the observations may offer a way to focus the parameterization of these effects.

Recognition of the existence of a spectrum of sinking rates already provides a step forward in the understanding of the controls on carbon transfer to the deep sea, although many of the insights have been previously explored based on two end-member models (Armstrong et al., 2002; Lutz et al., 2002). Fig. 5 illustrates some of the interesting aspects based on our VERTIGO K2-1 sinking-rate results. It shows the POC flux as a function of depth for each sinking-rate fraction (10 fractions are shown, combining the cups #10 and #11 fractions to make a single 2–6 m d^{-1} fraction) assuming first-order remineralization (at the rate, k, of 25% d^{-1}). The total POC flux, F, is then represented by the sum of

these fractions:

$$F(z) = \sum_i f_i \exp\left(-\frac{kz}{s_i}\right),$$

in which the f_i represent the fractional contributions to the flux from the s_i sinking-rate classes (as determined at some depth z^0). A remineralization rate of $\sim 25 \pm 5\%$ per day is required to mimic the profile of attenuation of the total POC flux with depth suggested by fitting other VERTIGO trap fluxes at 150, 300, and 500 m depth to a power law (Martin et al., 1987):

$$F(z) = \left(\frac{z}{z_0}\right)^{-b},$$

which yielded a b value of 0.51 (Buesseler et al., 2007a, b). But at this remineralization rate, slow-sinking particles would be quickly removed by remineralization and should not be present as an important component of the flux (Fig. 5). Thus, their presence suggests these particles are probably formed at depth by disaggregation of other particles, or by biological processes. This conclusion is emphasized by recent evidence that slow-sinking particles may be remineralized more rapidly than fast-sinking particles (Goutx et al., 2007), and is in keeping with the suggestions from carbon balances and fecal pellet studies that zooplankton are actively modifying sinking flux at depth at K2 (Steinberg et al., 2008a; Wilson et al., 2008). It is also worth noting that the remineralization rate of 25% is high in comparison to estimates of 1–10% from incubation studies (Panagiotopoulos et al., 2002; Pantoja et al., 2004), probably again reflecting the importance of zooplankton in flux attenuation. Fig. 5 also suggests that the spectrum of sinking rates should vary with depth, but first observations from MedFlux suggest that such variations are small if present at all (Armstrong, 2006). Finally, Fig. 5 emphasizes that fast-sinking particles are particularly important in the delivery of POC to the deep ocean, although such particles of course can be formed not only at the surface but also at mesopelagic depths. Much more sophisticated models of mesopelagic particle fluxes have been developed (Stemmann et al., 2004a, b), and an objective beyond the scope of this paper is the comparison of all the VERTIGO observations to those efforts.

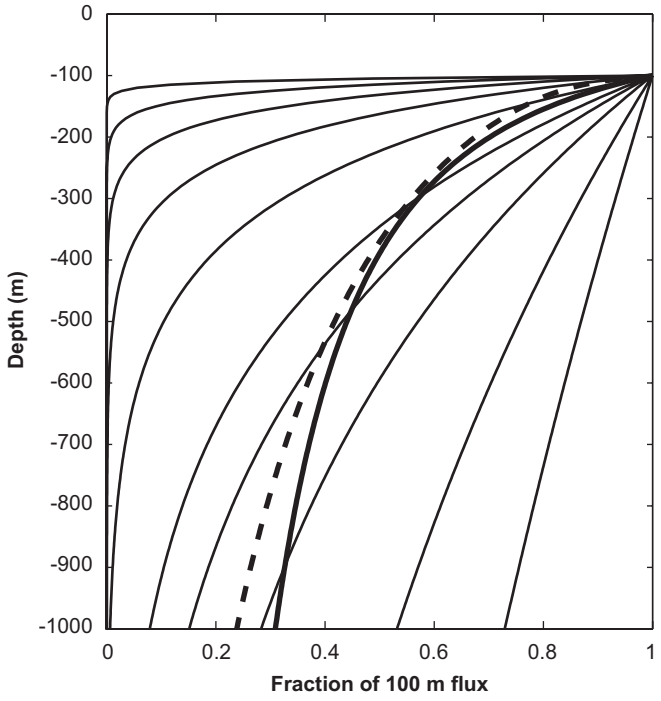

Fig. 5. The influence of a distribution of sinking rates on flux attenuation with depth. The thin lines show the flux attenuation for 10 individual sinking-rate fractions (right to left for fastest ($820\,m\,d^{-1}$) to slowest sinking ($2\,m\,d^{-1}$)) for a first-order 25% per day remineralization rate. Summing these contributions according to the POC flux in each fraction for the K2-1 IRS deployment (Fig. 4) yields a total flux (dashed line) similar to the power-law parameterization (thick line) of flux attenuation fitted to K2 total sinking flux results at 150, 300, and 500 m depth from neutrally buoyant and surface-suspended traps during VERTIGO (Buesseler et al., 2007a, b).

5. Concluding perspectives

Sinking rates of marine particles display sufficient range to be important in the control of particle transport to the deep sea. Whether the distribution of these rates varies significantly from place to place or time to time in the ocean remains an open question, and determining *in situ* mesopelagic sinking rates remains a daunting task. The IRS trap seems useful if imperfect for this purpose. Measurements of other particle properties such as size are unlikely to be a sufficient substitute, given the wide range of particle sizes within a sinking-rate fraction in our observations, and the100-fold range of sinking rates within a given size fraction as observed in compilations (especially for the important size range from 100 to 1000 μm; (Stemmann et al., 2004b; Khelifa and Hill, 2006).

Acknowledgments

Thanks to Lee Bond of Prime Focus, Inc., for quality craftsmanship on a tight timetable, Brian Popp (U. Hawaii) for generous help to prepare for the ALOHA voyage, Lisette Robertson (ACE) for logistics and onboard assistance during the 2004 voyage, and the captains and crew of the R.V. *Kilo Moana* (2004) and R.V. *Roger Revelle* (2005). Funding was provided by the US National Science Foundation (Chemical and Biological Oceanography) and the Australian Commonwealth Cooperative Research Centres Program. Cindy Lee, Rob Armstrong, Michael Peterson, and Kirk Cochran generously shared MedFlux IRS trap results prior to publication. We thank Cindy Lee and two anonymous referees for their extensive and insightful efforts that improved the paper. This paper is dedicated to Mary Silver and Scott Fowler, pioneers in the study of the upper ocean's biological pump.

References

Alldredge, A.L., 1998. The carbon, nitrogen and mass content of marine snow as a function of aggregate size. Deep-Sea Research I 45, 529–541.
Alldredge, A.L., Gotschalk, C., 1988. In situ settling behavior of marine snow. Limnology and Oceanography 33 (3), 339–351.
Antia, A.N., 2005. Solubilization of particles in sediment traps: revising the stoichiometry of mixed layer export. Biogeosciences 2, 189–204.
Armstrong, R.A., Lee, C., Hedges, J.I., Honjo, S., Wakeham, S.G., 2002. A new mechanistic model for organic carbon fluxes in the ocean based on the quantitative association of POC with ballast minerals. Deep-Sea Research II 49, 219–236.
Armstrong, R.A., 2006. Optimality-based modeling of nitrogen allocation and photoacclimation in photosynthesis. Deep-Sea Research II 53, 513–531.
Asper, V.L., 1987. Measuring the flux and sinking speed of marine snow aggregates. Deep-Sea Research 34 (1), 1–17.
Asper, V.L., Smith, W.O.J., 2003. Abundance, distribution and sinking rates of aggregates in the Ross Sea, Antarctica. Deep-Sea Research I 50, 131–150.
Asper, V.L., Deuser, W.G., Knauer, G.A., Lohrenz, S.E., 1992. Rapid coupling of sinking particle fluxes between surface and deep ocean waters. Nature 357, 670–672.
Boyd, P.W., Trull, T.W., 2006. Understanding the export of marine biogenic particles: is there consensus? Progress in Oceanography 4, 276–312.
Boyd, P.W., Gall, M.P., Silver, M.W., Bishop, J.K.B., 2008. Quantifying the surface-subsurface biogeochemical coupling during the VERTIGO ALOHA and K2 studies. Deep-Sea Research II, this issue [doi:10.1016/j.dsr2.2008.04.010].
Broecker, W.S., Takahashi, T., 1978. The relationship between lysocline depth and in situ carbonate ion concentration. Deep-Sea Research 25, 65–95.

Buesseler, K.O., Steinberg, D.K., Michaels, A.F., Johnson, R.J., Andrews, J.E., Valdes, J.R., Price, J.F., 2000. A comparison of the quantity and composition of material caught in a neutrally buoyant versus surface-tethered sediment trap. Deep-Sea Research I 47, 277–294.

Buesseler, K., Bishop, J., Boyd, P., Casciotti, K., Dehairs, F., Lamborg, C., Siegel, D., Silver, M., Steinberg, D., Saito, S., Trull, T., Valdes, J., Van Mooy, B., 2006. What We Know From VERTIGO. ASLO-TOS-AGU Ocean Sciences Meeting Abstract, OS22H-02.

Buesseler, K.O., Antia, A.N., Chen, M., Fowler, S.W., Gardner, W.D., Gustafsson, O., Harada, K., Michaels, A.F., Rutgers van der Loeff, M., Sarin, M., Steinberg, D.K., Trull, T., 2007a. Estimating upper ocean particle fluxes with sediment traps: a progress report. Journal of Marine Research 65 (3), 345–416.

Buesseler, K.O., Lamborg, C.H., Boyd, P.W., Lam, P.J., Trull, T.W., Bidigare, R.R., Bishop, J.K.B., Casciotti, K.L., Dehairs, F., Elskens, M., Honda, M., Karl, D.M., Siegel, D., Silver, M., Steinberg, D., Valdes, J., Van Mooy, B., Wilson, S.E., 2007b. Revisiting carbon flux through the Ocean's twilight zone. Science 316 (5824), 567–570.

Buesseler, K.O., Trull, T.W., Steinberg, D.K., Silver, M.W., Siegel, D.A., Saitoh, S.-I., Lamborg, C.H., Lam, P.J., Karl, D.M., Jiao, N.Z., Honda, M.C., Elskens, M., Dehairs, F., Brown, S.L., Boyd, P.W., Bishop, J.K.B., Bidigare, R.R., 2008. VERTIGO (VERtical Transport In the Global Ocean): a study of particle sources and flux attenuation in the North Pacific. Deep-Sea Research II, this issue [doi:10.1016/j.dsr2.2008.04.024].

Deuser, W.G., 1996. Temporal variability of particle flux in the deep Sargasso Sea. In: Ittekkot, V., Schafer, P., Honjo, S., Depetris, P.J. (Eds.), Particle Flux in the Ocean. SCOPE. Wiley, New York, pp. 185–198.

Deuser, W.G., Brewer, P.G., Jickells, T.D., Commeau, R.F., 1983. Biological control of the removal of abiogenic particles from the surface ocean. Science 219, 388–391.

Diercks, A.-R., Asper, V.L., 1997. In situ settling speeds of marine snow aggregates below the mixed layer: Black Sea and Gulf of Mexico. Deep-Sea Research I 44, 385–398.

Dunne, J.P., Armstrong, R.A., Gnanadesikan, A., Sarmiento, J.L., 2005. Empirical and mechanistic models for the particle export ratio. Global Biogeochemical Cycles 19, GB4026, doi:10.1029/2004GB002390.

Ebersbach, F., Trull, T.W., 2008. Sinking particle properties from polyacrylamide gels during the KErguelen Ocean and Plateau compared Study (KEOPS): zooplankton control of carbon export in an area of persistent natural iron inputs in the Southern Ocean. Limnology and Oceanography 53, 212–224.

Fowler, S.W., Knauer, G.A., 1986. Role of large particles in the transport of elements and organic compounds through the oceanic water column. Progress in Oceanography 16, 147–194.

Francois, R., Honjo, S., Krishfield, R., Manganini, S., 2002. Factors controlling the flux of organic carbon to the bathypelagic zone of the ocean. Global Biogeochemical Cycles 16(4), doi:10.1029/2001GB001722.

Gardner, W.D., 2000. Sediment trap sampling in surface waters. In: Hanson, R.B., Ducklow, H.W., Field, J.G. (Eds.), The Changing Ocean Carbon Cycle: A Midterm Synthesis of the Joint Global Ocean Flux Study. International Geosphere-Biosphere Programme Book Series. Cambridge University Press, Cambridge, pp. 240–281.

Goutx, M., Wakeham, S.G., Lee, C., Duflos, M., Guigue, C., Liu, Z., la Moriceau, B., Sempere, R., Tedetti, M., Xue, J., 2007. Composition and degradation of marine particles with different settling velocities in the northwestern Mediterranean Sea. Limnology and Oceanography 52 (4), 1645–1664.

Gust, G., Bowles, W., Giordano, S., Huttel, M., 1996. Particle accumulation in a cylindrical sediment trap under laminar and turbulent steady flow: an experimental approach. Aquatic Sciences 58 (4), 297–326.

Honda, M.C., Kawakami, H., Sasaoka, K., Watanabe, S., Dickey, T., 2006. Quick transport of primary produced organic carbon to the ocean interior. Geophysical Research Letters 33, L16603.

Honjo, S., 1996. Fluxes of particles to the interior of the open oceans. In: Ittekkot, V., Schafer, P., Honjo, S., Depetris, P.J. (Eds.), Particle Flux in the Ocean. Wiley, pp. 91–154.

Honjo, S., Francois, R., Manganini, S., Dymond, J., Collier, R., 2000. Particle fluxes to the interior of the Southern Ocean in the Western Pacific sector along 170W. Deep-Sea Research II 47 (15–16), 3521–3548.

Ittekkot, V., 1993. The abiotically driven biological pump in the ocean and short-term fluctuations in atmospheric CO_2 contents. Global Planetary Change 8, 17–25.

Ittekkot, V., Haake, V., Bartsch, M., Nair, R.R., Ramaswamy, V., 1992. Organic carbon removal in the sea: the continental connection. In: Summerhayes, C.P., Prell, W.L., Emeis, K.C. (Eds.), Upwelling Systems: Evolution Since the Early Miocene. Geological Society of America, pp. 167–176.

Jackson, G.A., 1995. Comparing observed changes in particle size spectra with those predicted using coagulation theory. Deep-Sea Research II 42 (1), 159–184.

Jahnke, R.A., 1996. The global ocean flux of particulate organic carbon: areal distribution and magnitude. Global Biogeochemical Cycles 10 (1), 71–88.

Karl, D.M., Christian, J.R., Dore, J.E., Hebel, D.V., Letelier, R.M., Tupas, L.M., Winn, C.D., 1996. Seasonal and interannual variability in primary production and particle flux at Station ALOHA. Deep-Sea Research II 43 (2–3), 539–568.

Khelifa, A., Hill, P.S., 2006. Models for effective density and settling velocity of flocs. Journal of Hydraulic Research 44 (3), 390–401.

Klaas, C., Archer, D.E., 2002. Association of sinking organic matter with various types of mineral ballast in the deep sea: implications for the rain ratio. Global Biogeochemical Cycles 16 (4).

Koeve, W., 2002. Upper ocean carbon fluxes in the Atlantic Ocean: the importance of the POC:PIC ratio. Global Biogeochemical Cycles 16 (4), 1056.

Lamborg, C.H., Buesseler, K.O., Valdes, J., Bertrand, C.H., Bidigare, R., Manganini, S., Pike, S., Steinberg, D., Trull, T., Wilson, S., 2008. The flux of bio- and lithogenic material associated with sinking particles in the mesopelagic "Twilight Zone" of the northwest and north central Pacific Ocean. Deep-Sea Research II, this issue [doi:10.1016/j.dsr2.2008.04.011].

Lee, D.-K., Niiler, P.P., 2005. The energetic surface circulation patterns of the Japan/East Sea. Deep-Sea Research II 52, 1547–1563.

Lundsgaard, C., 1995. Use of a high viscosity medium in studies of aggregates. In: Floderus, S., Heisakanen, A.-S., Oleson, M., Wassman, P. (Eds.), Sediment Trap Studies in the Nordic Countries 3. Proceedings of the Symposium on Seasonal Dynamics of Planktonic Ecosystems and Sedimentation in Coastal Nordic Waters. Nurmiprint, Oy., pp. 141–152.

Lutz, M., Dunbar, R., Caldeira, K., 2002. Regional variability in the vertical flux of particulate organic carbon in the ocean interior. Global Biogeochemical Cycles 16 (3), 11-1–11-18.

MacIntyre, S., Alldredge, A.L., Gotschalk, C.C., 1995. Accumulation of marine snow at density discontinuities in the water column. Limnology and Oceanography 40 (3), 449–468.

Martin, J.H., Knauer, G.A., Karl, D.M., Broenkow, W.W., 1987. VERTEX: carbon cycling in the Northeast Pacific. Deep-Sea Research 34, 267–285.

Michaels, A.F., Knap, A.H., 1996. Overview of the US JGOFS Bermuda Atlantic Time-series Study and the Hydrostation S Program. Deep-Sea Research 43, 157–198.

Noji, T.T., Estep, K.W., MacIntyre, F., Norrbin, F., 1991. Image analysis of faecal material grazed upon by three species of copepods: evidence for coprorhexy, coprophagy, and coprochaly. Journal of the Marine Biological Association of the United Kingdom 71, 46–480.

Oschlies, A., Kahler, P., 2004. Biotic contribution to air–sea fluxes of CO_2 and O_2 and its relation to new production, export production, and net community production. Global Biogeochemical Cycles 18 (GB1015).

Panagiotopoulos, C., Sempere, R., Obernosterer, I., Striby, L., Goutx, M., Van Wambeke, F., Gautier, S., Lafont, R., 2002. Bacterial degradation of large particles in the southern Indian Ocean using in vitro incubation experiments. Organic Geochemistry 33, 985–1000.

Pantoja, S., Sepulveda, J., Gonzalez, H.E., 2004. Decomposition of sinking proteinaceous material during fall in the oxygen minimum zone off northern Chile. Deep-Sea Research I 51, 55–70.

Passow, U., 2004. Switching perspectives: do mineral fluxes determine particulate organic carbon fluxes or vice versa? Geochemistry, Geophysics, Geosystems 5 (4), Q04002 doi:1029/2003GC000670.

Passow, U., De La Rocha, C., 2006. The accumulation of mineral ballast on organic aggregates. Global Biogeochemical Cycles 20, GB1013.

Passow, U., Alldredge, A.L., Logan, B.E., 1994. The role of particulate carbohydrate exudates in the flocculation of diatom blooms. Deep-Sea Research I 41, 335–357.

Peterson, M.L., Hernes, P.J., Thoreson, D.S., Hedges, J.I., Lee, C., Wakeham, S.G., 1993. Field evaluation of a valved sediment trap. Limnology and Oceanography 38 (8), 1741–1761.

Peterson, M.L., Wakeham, S.G., Lee, C., Askea, M.A., Miquel, J.C., 2005. Novel techniques for collection of sinking particles in the ocean and determining their settling rates. Limnology and Oceanography Methods 3, 520–532.

Peterson, T.D., Whitney, F.A., Harrison, P.J., 2005. Macronutrient dynamics in an anticyclonic mesoscale eddy in the Gulf of Alaska. Deep-Sea Research II 52, 909–932.

Pilskaln, C.H., Lehmann, C., Paduan, J.B., Silver, M.W., 1998. Spatial and temporal dynamics in marine aggregate abundance, sinking rate, and flux: Monterey Bay, central California. Deep-Sea Research II 45, 1803–1837.

Queguiner, B., 2001. Biogenic silica production in the Australian sector of the Sub-Antarctic Zone of the Southern Ocean in late summer 1998. Journal of Geophysical Research 106 (C12), 31,627–31,636.

Sarmiento, J.L., Orr, J.C., 1991. Three-dimensional simulations of the impact of Southern Ocean nutrient depletion on atmospheric CO_2 and ocean chemistry. Limnology and Oceanography 36, 1928–1950.

Silver, M.W., Gowing, M.M., 1991. The "particle" flux: origins and biological components. Progress in Oceanography 26, 75–113.

Steinberg, D.K., Van Mooy, B.A.S., Buesseler, K.O., Boyd, P.W., Kobari, T., Karl, D.M., 2008a. Bacterial versus zooplankton control of sinking particle flux in the ocean's twilight zone. Limnology and Oceanography 53 (4), 1327–1338.

Steinberg, D.K., Cope, J.S., Wilson, S.E., Kobari, T., 2008b. A comparison of mesopelagic zooplankton community structure in the subtropical and subarctic North Pacific Ocean. Deep-Sea Research II, this issue [doi:10.1016/j.dsr2.2008.04.025].

Stemmann, L., Jackson, G.A., Gorsky, G., 2004a. A vertical model of particle size distributions and fluxes in the midwater column that includes biological and physical processes—Part II: Application to a three year survey in the NW Meditteranean Sea. Deep-Sea Research I 51, 885–908.

Stemmann, L., Jackson, G.A., Ianson, D., 2004b. A vertical model of particle size distributions and fluxes in the midwater column that includes biological and physical processes—Part I: Model formulation. Deep-Sea Research I 51, 865–884.

Suess, E., 1980. Particulate organic carbon flux in the oceans-surface productivity and oxygen utilization. Nature 288, 260–263.

Turner, J.T., 2002. Zooplankton fecal pellets, marine snow and sinking phytoplankton blooms. Aquatic Microbial Ecology 27, 57–102.

Volk, T., Hoffert, M.I., 1985. Ocean carbon pumps: analysis of relative strengths and efficiencies in ocean-driven atmospheric CO_2 changes. In: Sundquist, E., Broecker, W.S. (Eds.), The Carbon Cycle and Atmospheric CO_2: Natural Variations Archean to Present. Geophysical Monograph. AGU, Washington, DC, pp. 99–110.

Wilson, S.E., Steinberg, D.K., Buesseler, K.O., 2008. Changes in fecal pellet characteristics with depth as indicators of zooplankton repackaging of particles in the mesopelagic zone of the subtropical and subarctic North Pacific Ocean. Deep-Sea Research II, this issue [doi:10.1016/j.dsr2.2008.04.019].

Yamanaka, Y., Tajika, E., 1996. The role of the vertical fluxes of particulate organic matter and calcite in the oceanic carbon cycle: studies using an ocean biogeochemical general circulation model. Global Biogeochemical Cycles 10, 361–382.